Experimental evidence for carbonyl–π electron cloud interactions†

Julien E. Gautrot,*[a] Philip Hodge,*[a] Domenico Cupertino[b] and Madeleine Helliwell[a]

Received (in Montpellier, France) 20th June 2006, Accepted 22nd August 2006
First published as an Advance Article on the web 12th September 2006
DOI: 10.1039/b608628d

In this work we present some experimental evidence of the existence of carbonyl–π electron cloud interactions. Such interactions are analogous to anion–π interactions, which have been predicted to be energetically favourable in the case of electron deficient aromatic rings. UV-Visible spectroscopy and cyclic voltammetry results obtained for 9,10-anthraquinone, 1,1′-bis-9,10-anthraquinone, poly(9,10-anthraquinone-1,4-diyl) and other 1,4-diaryl substituted anthraquinone derivatives are described. It was found that the steric hindrance occurring between the carbonyl groups and the adjacent aromatic substituent forces the plane of the anthraquinone moiety and that of the aromatic substituent to adopt a nearly orthogonal conformation, resulting in relatively strong carbonyl–π interactions that affect both the UV-Vis absorption spectrum and the reduction potential of the compound. Moreover, in the case of thiophene substituted derivatives, the torsion angle between the anthraquinone moiety and its aromatic substituent is smaller and therefore carbonyl–π interaction effects are not observed in these compounds.

Introduction

Supramolecular structures are generally stabilized by a range of favourable non-bonding interactions, for example, hydrogen bonds and the π-stacking of aromatic rings. Understanding the various interactions is, amongst other things, crucial to the development of conjugated materials for electronic applications. In this article we present experimental evidence that supports the presence of favourable interactions between the oxygen atom of a carbonyl group and an aromatic ring.

In the course of our studies of high electron-affinity polymers we prepared a range of anthra-9,10-quinone-based polymers including poly(1,4-dianthraquinoyl) (**1**). Previous studies by Yamamoto *et al*. showed that the highest transition in the UV-Vis spectrum of **1** is shifted to lower energies compared to that of anthra-9,10-quinone (**2**).[1] They attributed this shift to an increase in the conjugation length along the polymer backbone. Our results reveal a similar trend in the evolution of the UV-Vis spectra. However, geometry optimization results obtained for 1,1′-bis-9,10-anthraquinone (**3**), a simple model of polymer **1**, together with the crystal structure of its diamino derivative **4**, revealed that the torsion angle between two anthraquinone units was close to 90° (85° from the geometry optimization results obtained for **3** and 83° from the crystal structure of **4**).[2] Such a large dihedral angle is expected due to the major steric hindrance introduced by the carbonyls of each anthraquinone moiety. This should prevent conjugation occurring along the polymer backbone of **1**. On the other hand, in such a conformation the oxygen atoms of the carbonyl groups are sufficiently close to the aromatic rings of the neighbouring moieties as to allow interactions to occur between the lone pairs on the oxygen atoms and the neighbouring π-system, *i.e*. carbonyl–π interactions are a possibility.

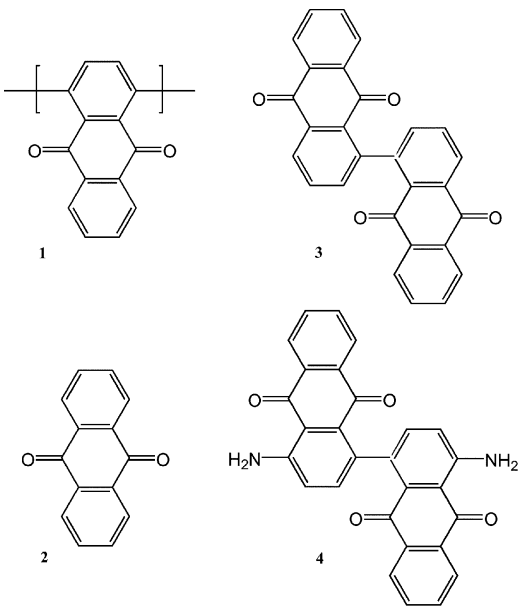

Results and discussion

Carbonyl–π interactions

Evidence of carbonyl–π interactions is scarce in the literature. Searches of the Cambridge Structural Database (CSD) show that carbonyl–π interactions are present in some protein crystals[3] as well as in some other organic crystals and between

[a] *Department of Chemistry, University of Manchester, Oxford Road, Manchester, UK M13 9PL. E-mail: juliengautrot@yahoo.fr; Philip.Hodge@manchester.ac.uk*
[b] *Avecia, Blackley, Manchester, UK*

† Electronic supplementary information (ESI) available: UV-Vis spectra of fully reduced **1**, **2** and **3**, UV-Vis spectra of models **5–8**, evolution of the CT band of model **7** with the dielectric constant of the solvent, CV traces of models **5–8** and crystallographic data for compounds **6** and **9**. See DOI: 10.1039/b608628d

aromatic analytes and silica supported polyacrylate derivatives (although in this latter case the exact nature of the interactions was not fully investigated).[4] In the case of electron rich aromatic rings the carbonyl–π interactions were found to be energetically favourable only with an edge on approach of the carbonyl, while a face approach was favoured with electron deficient aromatic rings.

Recent studies have shown that anion–π interactions exist. Examples of systems hosting such interactions have been found in the CSD and have been the subject of recent papers,[5] but most of the work on this subject still remains theoretical.[6] The interaction between π-deficient systems such as 1,3,5-triazine[6d] or hexafluorobenzene[6b,e,f] and anions (or even heteroatoms in molecules such as H_2O or HF) was found to be energetically favourable. The magnitude of such interactions is similar to what can be calculated (and observed) in the case of the much more studied cation–π rich systems.[6a] Moreover, energy minima were found to lie along the principal symmetry axis of the molecule with distances from the centroid typically falling between 2 and 3 Å.

A model of the carbonyl–π interaction can be extrapolated from the studies of anion–π interactions, although the systems differ in several parameters such as the distance and orientation of the carbonyl double bond with respect to the principal axis (or rather pseudo axis considering the loss of symmetry in our system) of the aromatic ring. Keeping this in mind, the carbonyl–π interaction can be predicted to be energetically favourable in the case of electron deficient aromatic rings and destabilising in the case of electron rich rings. Such a model is consistent with results reported in the literature that were briefly presented above.[3,4]

Unsubstituted anthraquinone derivatives

Now let us return to anthraquinone dimer **3** and polymer **1**. How can the carbonyl–π interaction account for the UV-Vis spectrum of **3** and its electrochemical behaviour? In which way is this interaction necessary to explain the experimental results observed? In order to answer these questions, it is necessary to make a simple assumption: the electron density around the carbonyl oxygen atoms is increased in the LUMO. Compared to the HOMO of neutral **3**, the carbonyl–π interaction will more strongly perturb the LUMO than it does to the HOMO.[6f] Electronic transitions being vertical, no molecular reorganisation has sufficient time to occur, so the geometry of the molecule is not modified and the main parameter that changes is the electron density near the oxygen of each carbonyl group. The effect of such a phenomenon is to modify the optical band gap. The direction of this change will depend on the nature of the aromatic substituent. In the case of **3** and, more generally, with electron deficient aromatic substituents, both the HOMO and LUMO are stabilised, but the LUMO is more stabilised than the HOMO, as it has just been explained. The optical band gap decreases, and the highest π–π* transition is red-shifted (Fig. 1). The trend is the opposite in the case of electron rich aromatic substituents.

The electrochemical behaviour will also be affected by the carbonyl–π interaction. During the reduction of the anthraquinone moiety, the electron density increases around the

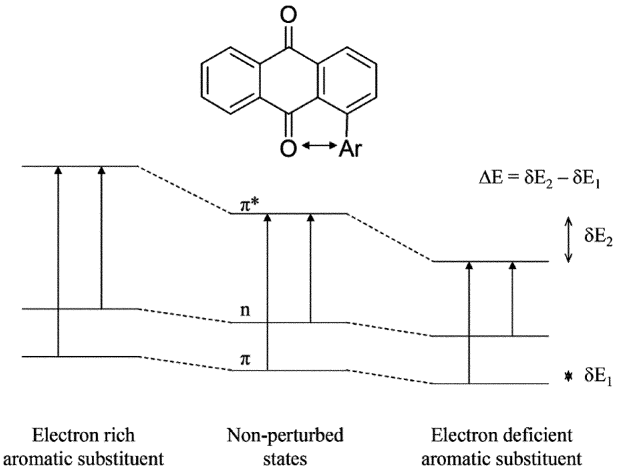

Fig. 1 Qualitative prediction of the evolution of UV-Vis spectra, considering carbonyl–π interactions only (all other effects are not included and may direct the overall changes).

oxygen atoms of the carbonyls. Any effect that will stabilise the semiquinone state (first reduced state in which one electron has been transferred) will shift the half-wave potential to a more positive potential. A carbonyl–π interaction will therefore shift the half-wave potential to more positive potentials in the case of electron deficient aromatic substituents, and to more negative potentials in the case of electron rich ones.

The UV-Vis spectra of polymer **1**, anthraquinone (**2**) and its dimer **3** in *N*-methylpyrrolidone (NMP) are presented in Fig. 2. Consider first the spectrum of **2**. Three transitions occur above 260 nm, consistent with the literature.[7] The two intense bands near 270 and 320 nm are known to be due to π–π* transitions with quinonoid and benzenoid characters, respectively.[8] The third band, near 400 nm, is very weak and is known to be due to the forbidden n–π* transition.

The highest π–π* transition is red-shifted from anthraquinone (**2**) to dimer **3**. The shift is about 12 nm, which corresponds to an apparent stabilization energy, Δ*E*, of

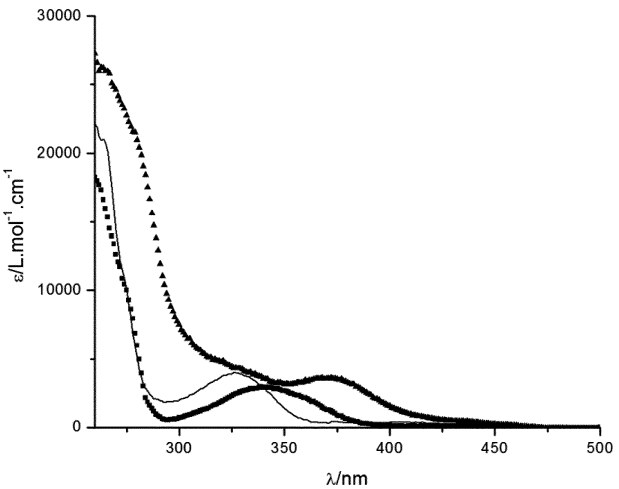

Fig. 2 UV-Vis spectra of 9,10-anthraquinone **2** (solid line), 1,1′-bis-9,10-anthraquinone **3** (squares) and poly(9,10-anthraquinone-1,4-diyl) **1** (triangles) in NMP.

3.1 kcal mol^{-1}. An even larger shift of 44 nm is observed in the case of polymer **1**, which corresponds to a ΔE of 10.4 kcal mol^{-1}. Such stabilization energies are comparable to the interaction energies reported for various halides interacting with hexafluorobenzene[5b,6a,e] (typically, near 13 kcal mol^{-1} for chloride and 18 kcal mol^{-1} for fluoride, depending on the method used for the calculations), although lower in magnitude. Obviously the present work is not a quantitative study, but these relatively small values of ΔE can be qualitatively rationalized. Firstly, the stabilization of the HOMO δE_1 tends to increase the optical band gap, which decreases ΔE (Fig. 1). Secondly, the position of the oxygen atom is not optimal for maximizing the interaction energy, since it is not placed along the axis passing through the centroid and orthogonal to the plane of the neighbouring aromatic ring.[6b,f]

The carbonyl–π interaction can also account for the differences observed in the cyclic voltammetry (CV) traces of **2** and **3** (see Fig. 3a and b). The CV trace of **2** in NMP shows two reversible reduction steps with respective half-wave potentials at −0.68 and −1.44 V (against Ag/AgCl), corresponding to two successive one-electron reductions, consistent with the literature.[9] The CV trace of **3** in NMP, however, displays four successive reduction steps (presumably of one-electron each). The first two are reversible and can be compared to the reduction of two isolated anthraquinone moieties: instead of displaying one two-electron reduction step, the two electrons are added successively. Moreover, the first reduction step occurs at slightly more positive potentials (−0.66 V) than for **2**. This is consistent with the hypothesis of a carbonyl–π interaction occurring in **3**. The second reduction step occurs at more negative potentials (−0.92 V), which is also consistent with the carbonyl–π interaction if one considers that the entity that is now reduced is an anthraquinone moiety substituted with an electron rich aromatic ring (Fig. 3c).

Now it is interesting to look at the UV-Vis spectra of **1**, **2** and **3** in their fully reduced states (in which each quinone moiety has been reduced to the corresponding dianion). For this purpose, solutions of **1**, **2** and **3** in NMP were treated with an excess of sodium hydrosulfite in alkali aqueous solution.[10] A UV-Vis spectrum was then recorded for each compound. All three UV-Vis spectra displayed two absorption bands,[10] presumably π–π*, as suggested by Carsky *et al.*,[11] and implied by the high extinction coefficients of these transitions. The position of the λ_{max} of the highest transition (near 500 nm) is almost unchanged when going from anthraquinone (**2**), to its dimer **3**, and then to polymer **1**. This result is predicted by the carbonyl–π interaction model. Indeed, for these dianions, the charge density centered on the oxygen atoms is very high in both the ground and excited states. Therefore, both of these states are stabilized in a similar way and the carbonyl–π interaction has no noticeable effect on the position of this transition. The hypothesis of a significant conjugation, despite the high torsion angle, between the anthraquinone units is not satisfactory since it does not explain the fact that the highest transition of the UV-Vis spectra of the fully reduced species does not shift when increasing the number of anthraquinone units in the chain.

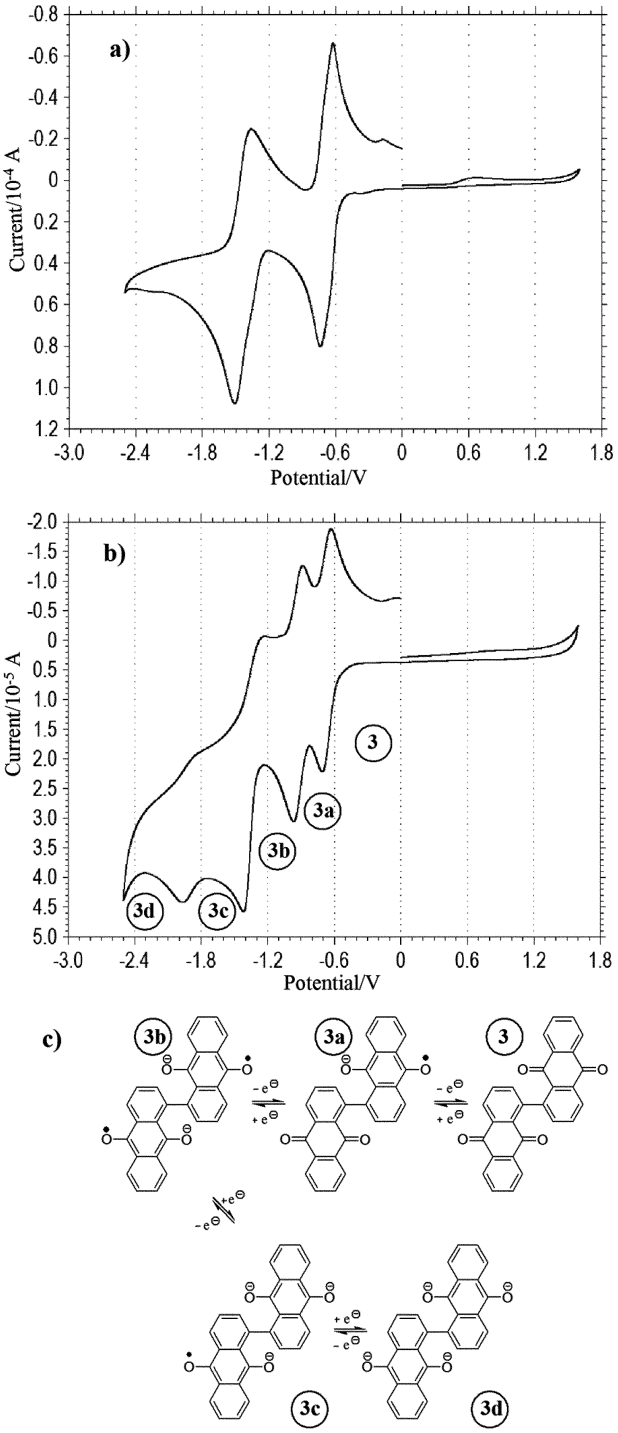

Fig. 3 CV traces obtained for (a) 9,10-anthraquinone **2** and (b) 1,1′-bis-9,10-anthraquinone **3** (3 mmol L^{-1}) in $TBAPF_6$ (0.1 mol L^{-1}) solution in degassed NMP (scan rate: 0.1 V s^{-1}), *vs.* Ag/AgCl; (c) successive reduction steps for dimer **3**.

Diaryl-substituted anthraquinone derivatives

In order to probe further the carbonyl–π interaction model, and check its validity for explaining the UV-Vis and electrochemical behaviour of 1-aryl and 1,4-diarylanthra-9,10-quinones, we decided to investigate the properties of other

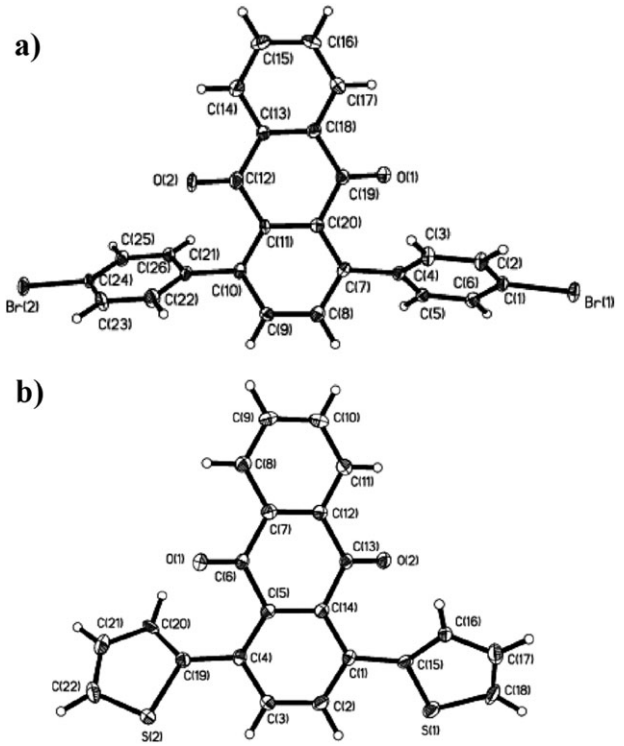

Fig. 4 X-Ray crystal structures of (a) 1,4-bis(4′-bromophenyl)-9,10-anthraquinone **9** and (b) 1,4-bisthien-2′-yl-9,10-anthraquinone **6**; the lower fraction disordered component has been omitted for clarity.

examples belonging to the latter family of molecules. For this purpose, models **5**, **6**, **7** and **8** were synthesized.[10] The spectroscopic and electrochemical properties of these molecules were found to depend greatly on their conformation. An X-ray crystal structure was obtained for model **6** and compound **9**, a dibromo derivative of model **5**. These results revealed that the torsion angle, ϕ, between the anthraquinone moiety and the aromatic substituent is still large in the case of phenyl substituents (59 and 69°) while it decreases significantly in the case of thienyl substituents (36 and 38°) (Table 1, Fig. 4), whereas the oxygen to ring-centroid distances are approximately equivalent for both compounds **6** and **9** (Table 1). This reduced torsion angle may be due to the smaller size of the sulfur atom compared to the aromatic CH, together with the larger angle between the linking single C–C bond and the adjacent aromatic double C=C bond (see angles C20–C19–C4 and C16–C15–C1 in Table 1), as well as potential chalcogen–chalcogen interactions between the oxygen of the carbonyl and the sulfur atom of the neighbouring thiophene ring,[12] given their relative proximity (the O1–S2A distance being 2.892 Å). The large torsion angle seen in **9** suggests that the carbonyl–π interaction is still relatively important in this molecule, while it is much weaker in the case of model **6**, for which the oxygen atoms of the anthraquinone carbonyls are not lying above the aromatic substituents.

Table 1 Important distances (Å), angles and dihedral angles (°) obtained for compounds **6** and **9** (standard deviations are in brackets)

Compound **6**		Compound **9**	
C20–C19–C4	130.6 (0.3)	C26–C21–C10	120.4 (0.3)
C16–C15–C1	129.4 (0.2)	C3–C4–C7	120.5 (0.3)
C5–C4–C19–C20	36.4 (0.5)	C11–C10–C21–C26	69.5 (0.5)
C14–C1–C15–C16	38.0 (0.4)	C3–C4–C7–C20	59.4 (0.5)
centroid–O1	2.649	centroid–O1	2.668
centroid–O2	2.660	centroid–O2	2.671

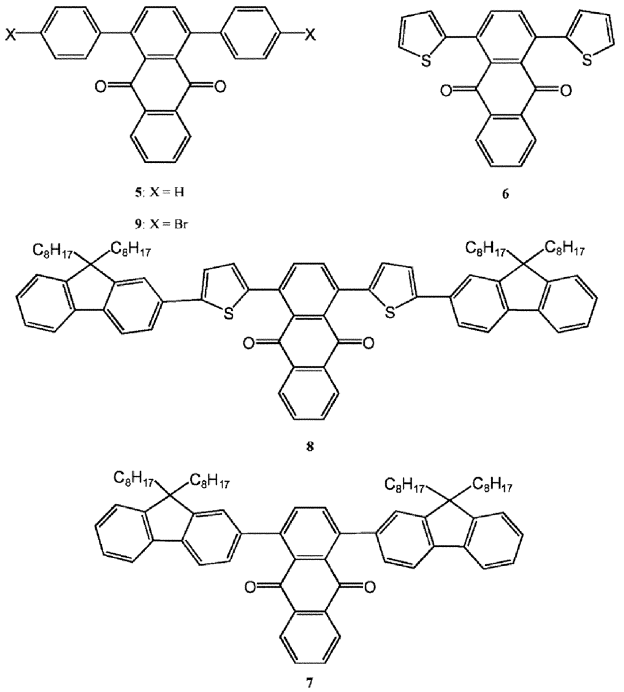

The UV-Vis spectra of models **5**, **6**, **7** and **8** were recorded in chloroform and compared to the spectrum of 9,10-anthraquinone **2** in the same solvent.[10] For all these models a weak broad transition could be observed at long wavelengths (with onsets of absorption ranging from near 400 nm for **5** to 600 nm for **8**), which was assigned to a charge transfer phenomenon. The study of the evolution of the position of this transition in various solvents revealed that it was sensitive to the dielectric constant of the milieu. At equal extinction coefficients, the transition is red-shifted in solvents displaying a high dielectric constant (for model **7** a red-shift of 9 nm can be observed when going from hexane to chloroform, for an extinction coefficient of 1000 L mol^{-1} cm^{-1}).[10] The second highest transition is ascribed to the highest π–π* transition. In the case of derivatives **5** and **7** (λ_{max} of 284 and 310 nm, respectively) this transition is blue-shifted compared to the highest π–π* of anthraquinone (**2**) (λ_{max} of 326 nm), while it is red-shifted in the case of thienyl derivatives **6** and **8** (λ_{max} of 326 and 367 nm, respectively). The blue shift observed for the highest π–π* of models **5** and **7** can be rationalized thanks to the carbonyl–π interaction: the presumably large torsion angle in these molecules allows a strong carbonyl–π interaction to take place, and the relatively high ionisation potential of the aromatic substituents means that this interaction is energetically destabilising. On the other hand, the reduction of the torsion angle in the case of thienyl derivatives will tend to reduce the carbonyl–π interaction and increase the extent of conjugation. Therefore, a red-shift is observed for the highest π–π* transition of these derivatives.

Table 2 Electrochemical results obtained for the model compounds

	$E_{1/2}{}^{c}$/mV	ΔE^{c}/mV	$1/2(E_{pa} + E_{pc})^{d}$/mV	ΔE^{d}/mV
5	−980	180	−1610	280
6	−850	200	−1430	260
7[a]	−970	390	−1710	150
8[b]	−910	840	−1920	490

[a] Results obtained for the different models in degassed anhydrous DCM solutions (electrolyte: $TBAPF_6$, 0.1 mol L^{-1}; scan rate: 0.1 V s^{-1}), *vs.* Ag/AgCl. [b] Quasi-irreversible peaks. [c] First reduction step. [d] Second reduction step.

The CV traces of 9,10-anthraquinone (**2**), as well as the different models, were recorded in DCM.[10] Table 2 gathers the results obtained. Quantitative electrochemical results within the anthraquinone family were rationalised using Hammet's theory (which relates the rate constant of a reaction to the nature of the substituents near the reactive center) and σ_p values.[9a,13] However, the results obtained for the various 1,4-diarylanthraquinones do not seem to follow any trend governed simply by Hammet's theory. The half-wave potential for the first reduction of **5** is shifted to more negative potentials compared to **2**, while it is shifted to more positive potentials in the case of **6**. In the latter case, the presence of a more extended conjugation decreases the aromaticity of one of the aromatic rings of the anthraquinone moiety. This tends to shift the half-wave potential to more positive potentials, since less energy is required to break the aromaticity of one of the benzene rings to form the anthracenoid moiety.[14] The loss of aromaticity of the substituted benzene ring of **6** is reflected by the variations in the C–C bond lengths within this ring.[10] On the other hand, such a phenomenon is not found in the case of **5**, since this molecule does not display any extended conjugation. Moreover the relatively important shift (−0.1 V) of the half-wave potential, compared to **2**, cannot be rationalised by simply using σ_p values. Comparison of the results obtained for **5** with those obtained for other derivatives, such as 2-methyl and 2,3-dimethyl-9,10-anthraquinone, using Hammet's theory show that a much smaller shift is expected (using a σ_p of −0.1 for phenyl groups). The carbonyl–π interaction explains this phenomenon well, since its effect, in the case of electron rich aromatic rings, is to shift the half-wave potential to more negative values. Unfortunately, the large ΔE (difference between the anodic and cathodic potentials, E_{pa} and E_{pc}) values obtained for models **7** and **8** do not allow the comparison of these results. This phenomenon is not fully understood yet.

Conclusion

To our knowledge, these results are the first to show that intramolecular carbonyl–π interactions do exist and that their effect on the UV-Vis spectra and electrochemical behaviour of the molecule can be rationalized qualitatively using theoretical calculations on anion–π systems. However, it is important to stress that this study remains qualitative. Molecular modeling of the models studied will help to rationalize the phenomenon quantitatively. Ultimately, the family of 1,4-diaryl-9,10-anthraquinone could be expanded further and could offer an opportunity to test the theoretical results obtained for anion–π systems.

Experimental

Methods and materials

For purifications with flash column chromatography Merck 9385 silica gel 60 (230–400 mesh) was used. Thin layer chromatography (TLC) was carried out using Merck silica gel (60–254 mesh) coated on PET plates. NMR spectra were recorded on a Varian Inova 300 MHz spectrometer (abbreviations used: s, singlet; d, doublet; t, triplet; q, quadruplet; m, multiplet; bp, broad peak; bd, broad doublet; bm, broad multiplet; obs, observed; req, required). FT-IR spectra were recorded on a Perkin Elmer spectrometer with a He/Ne 633 nm (<0.4 mW) laser. Mass spectrometry was carried out using a Micromass Trio 2000 instrument for EI/CI, a Micromass Platform instrument for electrospray and a Micromass ToF Spec 2E instrument for MALDI ToF. Melting points were measured using a Gallenkamp melting point apparatus. Elemental analysis was performed by the Microanalysis lab of the Department of Chemistry, University of Manchester. DSC measurements were carried out on a Seiko Instruments DSC 220G instrument. UV-Vis spectra were recorded using a Unicam UV 300 spectrometer (abbreviations used: sh, shoulder). Cyclic voltammograms were recorded using a CH Instruments Electrochemical Workstation. The working electrode was glassy carbon, the counter electrode was a platinum wire and the reference electrode was Ag/AgCl. All measurements were carried out under an argon atmosphere. Molecular modeling results were carried out by the Computational Chemistry Group at Avecia Research Centre, Blackley. All chemicals and solvents were purchased from Aldrich, Lancaster, Fluka, Avocado or Strem. They were used without further purification unless stated. $Pd(PPh_3)_4$[15] was synthesised as described in the literature.

General procedure for the preparation of 1,4-diaryl-9,10-anthraquinones

The bistriflate of 1,4-dihydroxy-9,10-anthraquinone or 1,4-bis(5′-bromothien-2′-yl)-9,10-anthraquinone (1.00 eq), aryl boronic acid or ester (2.00 eq) and palladium(0) tetrakis (triphenylphosphine) (3 mol%) were placed in a round-bottomed flask (3-neck, 100 mL), fitted with a condenser, under nitrogen. THF (40 mL, degassed with argon) and aqueous sodium carbonate (1.0 M, 15 mL, degassed with argon) were added *via* a septum. The mixture was heated under reflux overnight and poured onto aqueous hydrochloric acid (0.1 M, 200 mL). This aqueous phase was extracted with dichloromethane (2 × 50 mL), washed with water (3 × 50 mL), dried over magnesium sulfate, filtered off and the solvent evaporated under vacuum.

1,4-Diphenyl-9,10-anthraquinone (5). The title compound **5** was prepared from the bistriflate of 1,4-dihydroxy-9,10-anthraquinone (1.50 g, 3.47 mmol), phenylboronic acid (850 mg, 6.96 mmol), palladium(0) tetrakis(triphenylphosphine) (242 mg, 0.21 mmol), THF (40 mL, degassed with argon) and aqueous sodium carbonate (1.0 M, 15 mL, degassed with

argon). Recrystallisation from toluene afforded yellow crystals (1.12 g, 90%). Mp 109–110 °C; IR (KBr, cm^{-1}) 1670, 1540, 1317, 1245, 957, 756, 729 and 697; ^{1}H NMR ($CDCl_3$, ppm) δ 8.07 (2H; m; H-5), 7.69 (2H; m; H-6), 7.57 (2H; s; H-2), 7.52–7.42 (6H; m) and 7.36–7.30 (4H; m); ^{13}C NMR ($CDCl_3$, ppm) δ 127.1, 127.4, 128.5, 133.0, 134.1, 136.7, 141.4, 142.6, 144.3, 146.3, 184.3; MS (EI/CI) 361 g mol^{-1}, $C_{26}H_{16}O_2$ requires 360 g mol^{-1}; UV-Vis spectrum (chloroform, nm) λ_{max}, 265 (21 950; sh), 284 (8080; sh) and 323 (3550; sh).

1,4-Dithien-2′-yl-9,10-anthraquinone (6). The title compound **6** was prepared from the bistriflate of 1,4-dihydroxy-9,10-anthraquinone (1.50 g, 3.47 mmol), 2-thiopheneboronic acid (900 mg, 6.94 mmol) and palladium(0) tetrakis(triphenylphosphine) (242 mg, 0.21 mmol), THF (40 mL, degassed with argon) and aqueous sodium carbonate (1.0 M, 15 mL, degassed with argon). Recrystallisation from toluene gave red needles (0.87 g, 67%). Mp (DSC) 235–236 °C; IR (KBr, cm^{-1}) 1681, 1595, 1457, 1304, 1254, 929, 850, 829 and 723; ^{1}H NMR ($CDCl_3$, ppm) δ 8.10 (2H; m; H-5), 7.71 (2H; m; H-6), 7.68 (2H; s; H-2), 7.45 (2H; d, J = 5.1 Hz; H-3′), 7.15 (2H; dd, J = 3 and 5 Hz; H-4′) and 7.06 (2H; d, J = 3 Hz; H-5′); ^{13}C NMR ($CDCl_3$, ppm) δ 126.3, 126.5, 127.1, 127.4, 134.1, 134.2, 137.1, 137.5, 142.8 and 183.9; MS (EI/CI) 372 g mol^{-1}, $C_{22}H_{12}O_2S_2$ requires 372 g mol^{-1}; microanalysis: calc: C, 70.9%, H, 3.3%, S, 17.2%; found: C, 70.1%, H, 2.9%, S, 16.1%; UV-Vis spectrum (chloroform, nm) λ_{max}, 326 (10 880), 364 (4000; sh).

1,4-Bis(9′,9′-dioctylfluoren-2′-yl)-9,10-anthraquinone (7). The title compound **7** was prepared from the bistriflate of 1,4-dihydroxy-9,10-anthraquinone (159 mg, 0.37 mmol), 9,9-dioctylfluorene-2-pinacolboronic ester (400 mg, 0.77 mmol), palladium(0) tetrakis(triphenylphosphine) (44 mg, 0.04 mmol), THF (10 mL, degassed with argon) and aqueous sodium carbonate (1.0 M, 5 mL, degassed with argon). Chromatography (silica, petroleum ether/DCM 90/10) afforded an orange oil that crystallises slowly in the refrigerator (273 mg, 75%). Mp (DSC) 76.3 °C; IR (KBr, cm^{-1}) 2925, 2853, 1676, 1463, 1457, 1445, 1317, 1271, 1244, 825 and 739; ^{1}H NMR ($CDCl_3$, ppm) δ 8.02 (2H; dd, J = 3 and 6 Hz; H-5), 7.82 (2H; d, J = 8 Hz), 7.76 (2H; m), 7.68 (2H; s; H-2), 7.67 (2H; dd, J = 3 and 6 Hz; H-6), 7.40–7.31 (8H; m), 7.24 (2H; m), 1.96 (8H; m), 1.29–1.00 (40H; m), 0.81 (12H; t, J = 7.0 Hz; H-8″), 0.77–0.59 (8H; m); ^{13}C NMR ($CDCl_3$, ppm) δ 14.4, 22.9, 24.1, 29.5, 29.6, 30.5, 32.1, 40.8, 55.4, 119.9, 120.9, 123.0, 123.6, 126.6, 126.8, 127.0, 127.3, 133.6, 133.8, 134.6, 136.5, 140.5, 141.3, 144.7, 150.8, 151.3 and 184.2; MS (MALDI) 986 g mol^{-1}, $C_{72}H_{88}O_2$ requires 986 g mol^{-1}; microanalysis: calc: C, 87.7%, H, 9.0%; found: C, 87.5%, H, 9.5%; UV-Vis spectrum (chloroform, nm) λ_{max}, 268 (63 900), 303 (29 100), 310 (28 000; sh), 362 (3700; sh).

Model compound (8). The title compound **8** was prepared from 1,4-bis(5′-bromothien-2′-yl)-9,10-anthraquinone (250 mg, 0.47 mmol), 9,9-dioctylfluorene-2-pinacolboronic ester (421 mg, 0.98 mmol), palladium(0) tetrakis(triphenylphosphine) (55 mg, 0.05 mmol), THF (40 mL, degassed with argon) and aqueous sodium carbonate (1.0 M, 15 mL, degassed with argon). Purification by chromatography (silica, petroleum ether : DCM 90 : 10) afforded a dark red oil (395 mg, 73%). IR (NaCl, cm^{-1}) 2926, 2853, 1676, 1654, 1560, 1541, 1457, 1307, 1247, 1076, 921, 799 and 738; ^{1}H NMR ($CDCl_3$, ppm) δ 8.17 (2H; dd, J = 3 and 6 Hz; H-5), 7.77 (2H; s; H-2), 7.75 (2H; dd, J = 3 and 6 Hz; H-6), 7.72 (4H; m), 7.65 (4H; m), 7.43 (2H; d, J = 4 Hz; H-3′), 7.34 (6H; m), 7.10 (2H; d, J = 4 Hz; H-4′), 2.02 (8H; t, J = 8 Hz; H-1′), 1.31–1.00 (40H; m), 0.82 (12H; t, J = 7 Hz; H-8‴) and 0.66 (8H; m); ^{13}C NMR ($CDCl_3$, ppm) δ 14.4, 22.9, 24.1, 29.5, 30.4, 32.1, 40.8, 53.7, 55.5, 120.0, 120.2, 120.3, 123.1, 125.0, 127.1, 127.2, 127.4, 127.9, 133.3, 134.2, 134.3, 137.0, 137.5, 140.9, 141.1, 141.7, 146.3, 151.2, 151.7 and 184.0 (30 obs, 32 req); MALDI 1150 g mol^{-1}, $C_{80}H_{92}O_2S_2$ requires 1150 g mol^{-1}; microanalysis: calc: C, 83.6%, H, 8.1%, S, 5.6%; found: C, 83.7%, H, 8.1%, S, 5.2%; UV-Vis spectrum (chloroform, nm)λ_{max}, 335 (54 100), 367 (32 700; sh) and 439 (5500; sh).

X-Ray crystallography

Single crystals suitable for X-ray crystallography of **6** and **9** were obtained from toluene, mounted in inert oil and transferred to the cold gas stream of the diffractometer.

Crystal data for 6. C_{22} H_{12} O_2 S_2, M = 372.44, monoclinic, a = 3.973(3), b = 10.960(7), c = 36.13(2) Å, β = 91.289(10)°, U = 1572.7(17) Å^3, T = 100 K, space group $P2_1/n$ (no. 14), Z = 4, μ(Mo Kα) = 0.353 mm^{-1}, 8807 reflections measured, 3244 unique (R_{int} = 0.042) which were used in all calculations. The atoms S2 and O20 were disordered over two sites whose occupancies were constrained to sum to unity, with the main fraction having a final occupancy of 0.91. The final $R(F)$ was 0.0425 using 3244 with $I > 2\sigma(I)$, wR_2 = 0.1048 (all data).

Crystal data for 9. C_{26} H_{14} Br_2 O_2, M = 518.19, triclinic, a = 5.8760(7), b = 9.9959(12), c = 17.790(2) Å, α = 102.163(2), β = 91.168(2), γ = 103.455(2)°, U = 990.8(2) Å^3, T = 100 K, space group $P\text{-}1$ (no. 2), Z = 2, μ(Mo Kα) = 4.113 mm^{-1}, 5802 reflections measured, 3963 unique (R_{int} = 0.029) which were used in all calculations. The final $R(F)$ was 0.038 using 3131 with $I > 2\sigma(I)$, wR_2 = 0.91 (all data).

CCDC reference numbers 618745–618746. For crystallographic data in CIF or other electronic format see DOI: 10.1039/b608628d

Chemical doping experiments

In a typical experiment, 9,10-anthraquinone **2** solution (4.6 × 10^{-5} mol L^{-1}) in NMP (UV-Vis spectroscopy grade) and a reductant solution of sodium hydrosulfite (4.6 × 10^{-3} mol L^{-1}) and sodium hydroxide (4.6 × 10^{-2} mol L^{-1}) in deionised water were degassed by gently bubbling argon through for 20 min. The 9,10-anthraquinone **2** solution (2 mL) was syringed into a spectroscopic cell (1 cm Spectrosil cell) fitted with a septum and further degassed for 5 min. A first UV-Vis spectrum was recorded at this stage. The reductant solution (0.05 mL) was added to the spectroscopic cell and the resulting mixture quickly shaken. Two further UV-Vis spectra were recorded just after addition of the reductant and after allowing the mixture to rest for 10 min. Finally, some reductant solution (0.05 mL) was added to the spectroscopic cell, the mixture shaken and a final UV-Vis spectrum recorded. The

reference used is an NMP solution in a matched cell. Identical amounts of reductant were added each time.

Acknowledgements

We thank Prof. S. Faulkner for his help with the UV-Vis spectroscopy and his patient discussion about photophysics. We also thank Dr P. Mackie for the molecular modeling results. This work was fully funded by Avecia Ltd, Blackley, UK.

References

1 (*a*) T. Yamamoto and H. Etori, *Macromolecules*, 1995, **28**, 3371; (*b*) T. Yamamoto, Y. Muramatsu, B.-L. Lee, H. Kokubo, S. Sasaki, M. Hasegawa, T. Yagi and K. Kubota, *Chem. Mater*., 2003, **15**, 4384.
2 (*a*) Work of Dr P. Mackie, Avecia Ltd, unpublished results; (*b*) K. Ogawa and H. J. Scheel, *Z. Kristallogr*., 1969, **130**, 405.
3 (*a*) K. A. Thomas, G. M. Smith, T. B. Thomas and R. J. Feldmann, *Proc. Natl. Acad. Sci. U. S. A*., 1982, **79**, 4843; (*b*) C.-Y. Kim, P. P. Chandra, A. Jain and D. W. Christianson, *J. Am. Chem. Soc*., 2001, **123**, 9620.
4 (*a*) A. Gambaro, P. Ganis, F. Manoli, A. Polimeno, S. Santi and A. Venzo, *J. Organomet. Chem*., 1999, **583**, 126; (*b*) H. Ihara, S. Uemura, S. Okazaki and C. Hirayama, *Polym. J. (Tokyo)*, 1998, **30**, 394.
5 (*a*) P. De Hoog, P. Gamez, I. Mutikainen, U. Turpeinen and J. Reedijk, *Angew. Chem., Int. Ed*., 2004, **43**, 5815; (*b*) D. Quinonero, C. Garau, C. Rotger, A. Frontera, P. Ballester, A. Costa and P. M. Deya, *Angew. Chem., Int. Ed*., 2002, **41**, 3389.
6 (*a*) C. Garau, A. Frontera, D. Quinonero, P. Ballester, A. Costa and P. M. Deya, *Chem. Phys. Lett*., 2004, **392**, 85; (*b*) C. Garau, D. Quinonero, A. Frontera, P. Ballester, A. Costa and P. M. Deya, *New J. Chem*., 2003, **27**, 211; (*c*) C. Garau, D. Quinonero, A. Frontera, A. Costa, P. Ballester and P. M. Deya, *Chem. Phys. Lett*., 2003, **370**, 7; (*d*) M. Mascal, A. Armstrong and M. D. Bartberger, *J. Am. Chem. Soc*., 2002, **124**, 6274; (*e*) D. Kim, P. Tarakeshwar and K. S. Kim, *J. Phys. Chem. A*, 2004, **108**, 1250; (*f*) I. Alkorta, I. Rozas and J. Elguero, *J. Org. Chem*., 1997, **62**, 4687; (*g*) I. Alkorta, I. Rozas and J. Elguero, *J. Am. Chem. Soc*., 2002, **124**, 8593.
7 (*a*) A. Navas Diaz, *J. Photochem. Photobiol., A*, 1990, **53**, 141; (*b*) J. Fabian and M. Nepras, *Collect. Czech. Chem. Commun*., 1980, **45**, 2605; (*c*) Z. Yoshida and F. Takabayashi, *Tetrahedron*, 1968, **24**, 933; (*d*) R. A. Morton and W. T. Earlam, *J. Chem. Soc*., 1941, 159; (*e*) R. H. Peters and H. H. Summer, *J. Chem. Soc*., 1953, 2101.
8 M. Nepras, J. Fabian and M. Titz, *Collect. Czech. Chem. Commun*., 1981, **46**, 20.
9 (*a*) P. Zuman, *Collect. Czech. Chem. Commun*., 1962, **27**, 2035; (*b*) J. Q. Chambers, Electrochemistry of quinones, in *The Chemistry of the Quinonoid Compounds*, ed. S. Patai and Z. Rappoport, Wiley, Toronto, 1988, p. 719.
10 See ESI.
11 P. Carsky, P. Hobza and R. Zahradnik, *Collect. Czech. Chem. Commun*., 1971, **36**, 1291.
12 V. I. Minkin and R. M. Minyaev, *Chem. Rev*., 2001, **101**, 1247.
13 (*a*) P. Zuman, *Collect. Czech. Chem. Commun*., 1962, **27**, 648; (*b*) E. Muller and W. Dilger, *Chem. Ber*., 1973, **106**, 1643.
14 (*a*) M. Buschel, C. Stadler, C. Lambert, M. Beck and J. Daub, *J. Electroanal. Chem*., 2000, **484**, 24; (*b*) G. J. Gleicher, D. F. Church and J. C. Arnold, *J. Am. Chem. Soc*., 1974, **96**, 2403.
15 D. R. Coulson, *Inorg. Synth*., 1972, **8**, 121.